Microwave Atom Chip Assembly System

Emmanuel Sampson
Ksenia (Kisa) Avrutina

Faculty Mentor: Seth Aubin, Department of Physics

Department of Physics, William & Mary

Williamsburg, Virginia

April 2026

Primary faculty mentor signature

Abstract

Microwave atom chips require broadband, low-reflection microwave inputs to narrow micrometer-scale on-chip traces. To achieve this, additional custom components must be added to the chip. This project is working to develop a device that would enable such additions to be made. This research focuses on the manipulation of a tapered dielectric-and-copper wedge that must be picked up, aligned to the chip's microwave trace, lowered, and held in place while an adhesive cures. A micromanipulation platform named *Scorpion* was constructed to achieve this. During development, three strategies were developed and compared: a vice-style claw, a tendon-inspired gripper, and a pneumatic pickup tool. These were integrated with translation-stage-based motion hardware selected for compatibility with the resolution requirements, spatial constraints, and low-cost in-lab assembly. The pneumatic approach performed best across pickup, placement, and hold-down. The tendon-inspired gripper demonstrated promise as a future adhesive tool. The final device assembled in this project incorporates a pneumatic pickup, coarse motion control from a gantry system, and fine motion control from translation stages. This approach yields control over alignment with longitudinal and lateral offsets and in-plane rotation during wedge placement. This thesis documents the design specification, subsystem architecture, failure modes, and next steps for constructing a desktop microwave atom-chip assembly system.

Acknowledgments

We thank our faculty mentor, Professor Seth Aubin, for his continued support and guidance throughout this project. This research was made possible by Professor Aubin's mentorship. We would also like to thank our fellow members of the Ultracold AMO laboratory for their technical assistance and discussions. We are further grateful to the William & Mary Physics Department and the Applied Research Center for granting us access to lab space and technical resources. Finally, we thank Professor Ran Yang for her invaluable feedback at each milestone of this project's construction.

Contribution Statement

Emmanuel Sampson was primarily responsible for conceptual designs, electronics implementation, and programming. Kisa Avrutina was primarily responsible for the mechanical design, CAD, and assembly of 3D-printed parts. Both authors participated in mechanical assembly, testing, evaluation of design iterations, and interpretation of results.

Contents

List of Figures

List of Tables

Chapter 1

Introduction

1.1 Motivation

Microwave circuits serve as groundbreaking solutions in electromagnetics, communication systems, and quantum sensing. Given their potential applications, researchers and industry professionals have endeavored to manufacture these boards using various methods. Conventional methods have the disadvantages of high cost and limited customization options. In the realm of quantum sensing, microwave circuits can be used to trap and channel atoms along a microwave trace. Use cases like this require specialized engineering for additional components and features that must be added to conventional planar circuits.

1.2 Problem Statement

High-precision customization of microwave circuit boards is needed to achieve low-reflection, broadband transmission for quantum sensing applications. The customization of microwave circuit boards is constrained by the lack of an accessible, user-driven assembly method. While microwave PCB transmission lines can carry large data volumes at higher speeds and with greater signal variability than conventional electronic circuits, they depend on precise alignment between amplifier inputs, coupling components, and the microwave traces to prevent discontinuities and reflections. Achieving broadband, low-reflection transmission (DC to 10 GHz or higher) is necessary to avoid the standing waves that arise from narrowband behavior. Broadband operation supports high-power drive, phase control, and microwave lattice formation, enabling precise manipulation of cold atoms or nanoparticles in quantum-technology applications. Broadband transmission can be achieved by adding tapered wedge components at the inputs of a planar circuit. These tapered wedges ensure gradual changes in geometric dimensions. Abrupt changes in trace or substrate dimensions introduce impedance and electromagnetic mode discontinuities, producing unwanted reflections and degrading transmission performance.

1.3 Project Objectives

The objective is to design a micromanipulation device for microwave atom chip assembly. This research aims to create a tool for component trapping, positioning, and adhesion. The effective placement of wedge components on microwave circuit boards requires precise positioning in the lateral (x), longitudinal (y), vertical (z), and rotational (α) directions (fig. 1.1). The final assembly system should incorporate control of all four relevant variables.

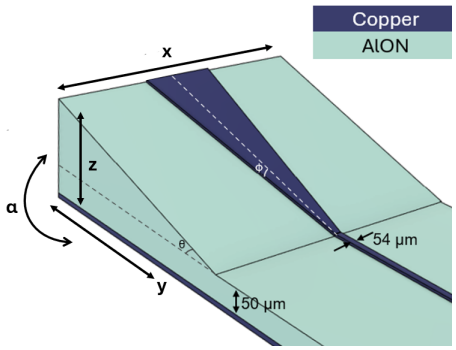

Figure 1.1: Tapered wedge and trace aligned with microwave transmission line, with directions of interest for positioning control labeled.

1.4 Scope and Constraints

This thesis covers the mechanical phase of the project: the placement requirements, the design iterations, and the motion-platform architecture, which determined the construction of the current device. The present platform does not include completed adhesive deposition, machine-vision alignment, or final microwave measurements on bonded assemblies.

The design was constrained to fit the system under an optical microscope, preserve the physical integrity of all manipulated components, and use low-cost laboratory hardware. The pickup tool had to fit under an optical microscope without blocking the view of the wedge and trace. The wedge and board could not be clamped destructively, so the manipulator had to place the part gently and then maintain hold-down in a manner that would simultaneously allow adhesive to be applied. Development also had to begin on larger practice hardware before translation to the smaller atom-chip geometry. The system described in this thesis used surrogate boards with traces approximately 200 µm wide, whereas the target atom-chip traces are approximately 54 µm wide. The larger practice pieces are less valuable and easier to work with, but still require precise, repeatable alignment and placement of the wedge components.

1.5 Thesis Organization

The thesis is organized as follows:

Chapter 1 outlined the motivation, problem statement, objectives, scope, and constraints of this project. Chapter 2 provides the theoretical background for both the microwave coupling and micromanipulation problems. Chapter 3 describes the micromanipulation system architecture, design iterations, and the test procedures used to compare them. Chapter 4 reports the observed behavior of each design and identifies the failure modes that most impacted performance. Chapter 5 evaluates those results against the functional requirements and discusses the trade-offs that drove the project toward a pneumatic pickup architecture. Chapter 5 also assesses and describes the efficiency of the final assembly with a pneumatic system. Chapter 6 summarizes the project's contributions and outlines the next engineering steps required to transform the current device into a more robust microwave atom chip assembly system.

Chapter 2

Theoretical Background

2.1 Literature Review

Devices engineered to capture and manipulate small parts are already common. Some examples include pick-and-place tools, surface-mounting devices, and surgical tweezers. Many recent efforts have focused on making such devices more lifelike in either their functionality or their interfaces. For example, in 2016, Hao et al. at Beihang University incorporated soft materials and dynamic pneumatic inflation and deflation of "fingers" to mimic the human hand in a robotic gripper device [1].

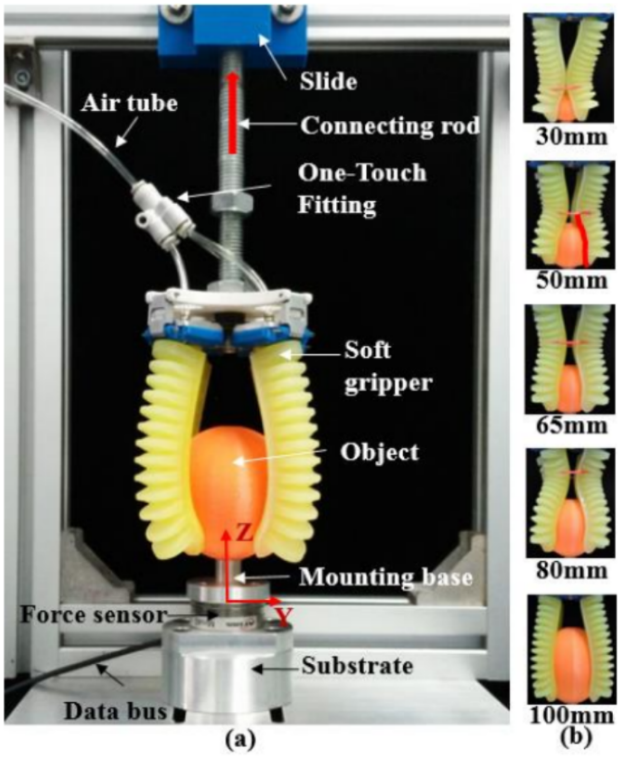

Figure 2.1: Image of hand-like pneumatic gripper by Hao et al. [1].

In 2020, Xie et al. from the same university explored an octopus-inspired gripper that combined soft materials with suction [2].

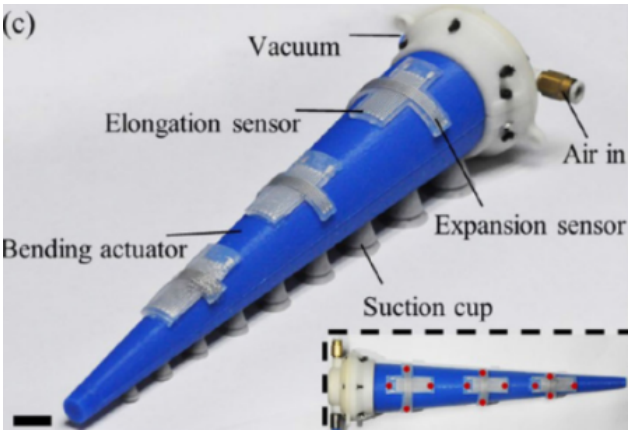

Figure 2.2: Image of suction gripper inspired by octopus tentacle by Xie et al. [2].

Such grippers, however, are built for the dimensions of tens or hundreds of millimeters. In the realm of micrometers, Moritoki et al. (2021) created 3D-printed micro-tweezers that use a compliant mechanism to manipulate microscopic biological samples [3]. This design, in trend with the previous two, uses the flexibility of its materials to achieve more precise tweezing.

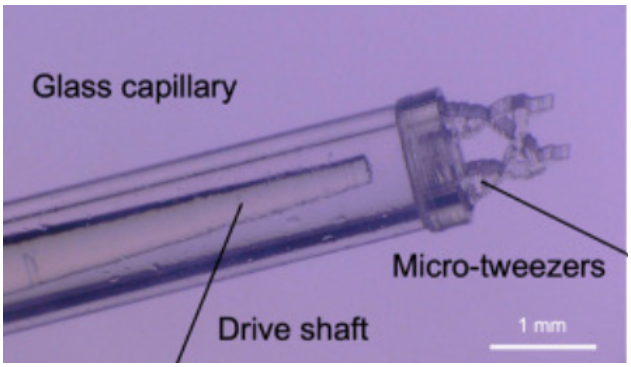

Figure 2.3: Image of 3D-printed compliant mechanism micro-tweezers by Moritoki et al. [3].

Abhilash Pandya (2023) translated this desire for more accessible, biologically-inspired technology into the interface of a da Vinci surgical robot [4]. Pandya uses the natural language of a ChatGPT-based model to improve the usability of a very complex robot that is otherwise challenging to master.

Another realm of micro-manipulation device engineering has explored the possibility of ultra-low-cost, homemade devices. Xu et al. (2021) present a 3D-printed, stepper-motor-driven, Arduino-operated single-cell micromanipulator [5]. For under $150, the group has achieved successful single-cell manipulation. Liao et al. (2022) even achieved atomic resolution imaging using a low-cost, homemade XYZ nanopositioner based on piezo actuators [6]. While none of these designs address the exact needs of customizable microwave circuit assembly, elements from each design serve as essential guides for the mechanisms needed to create Scorpion.

Beyond the mechanical design, the theoretical foundation of the microwave circuits that Scorpion is built to assemble is based upon the William & Mary PhD graduate William Miyahira's dissertation "Microwave Atom Chip Design" [7]. This paper describes the functionality and requirements for developing

microwave chips for the trapping and manipulation of ultra-cold atoms. This is otherwise known as atom interferometry.

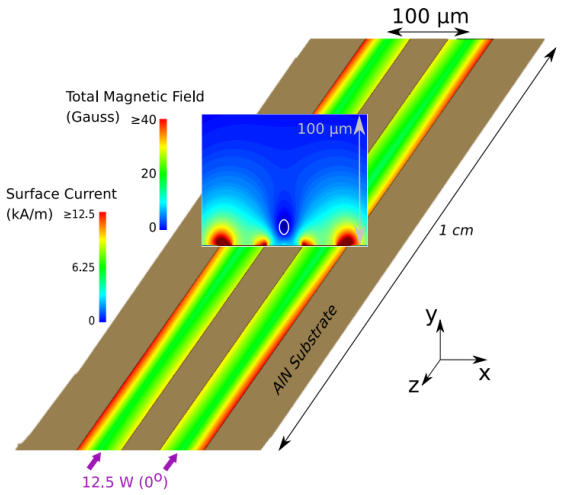

Figure 2.4: Image of microwave atom chip with atom trapping region circled. Figure taken from [7].

By creating this device, we hope to achieve perfect alignment among the amplifier inputs, coupling components, and board traces, as misalignment can cause discontinuities and reflections. Abrupt changes in trace or substrate geometry create impedance discontinuities (nominally 50 Ω) and alter electromagnetic modes, resulting in performance degradation. At microwave frequencies, geometry strongly determines field distributions and reflections. A microstrip transmission line's impedance Z_o depends on the relative permittivity of the substrate ε_r, the microstrip width w, the microstrip thickness z, and the substrate thickness h:

$$Z_o = \frac{87}{\sqrt{\varepsilon_r + 1.41}} \ln\left(\frac{7.48h}{w + 1.25z}\right) \tag{2.1}$$

Here, $z << w$ and $z << h$.

The system is designed for 50 Ω impedance. Even if impedance is nominally constant, a step change in geometry changes the mode size/shape and is reflective. To solve this, a wedge-like structure is proposed because it allows for smooth changes in geometry, preserving the width/height ratio while gradually transforming the mode as the trace narrows. This approach is non-standard, thus it calls for a unique engineering procedure.

2.1.1 Planar Circuit Limitations

The microwave trace is limited to a planar design due to the discontinuities in impedance and electromagnetic mode that arise due to changing geometrical dimensions of the trace or substrate. These discontinuities result in unwanted reflections, standing waves, and performance degradation at microwave frequencies. Accordingly, precision alignment is needed between the amplifier inputs, coupling components, and traces. A challenge arises in the coupling between standard coaxial connectors used

to feed in microwave signals and the microwave traces. Standard coaxial cables and connectors are designed with diameters suitable for RF frequencies, whereas the microwave traces, with a width of only 54 µm, are designed for much higher microwave frequencies. The difference in electromagnetic mode between the coaxial cable and the trace leads to significant reflections at the connecting point. In planar designs, narrow-band transmission results in a resonator. Reflections at the boundaries effectively "pin" the wave in place, creating a standing wave. For atom manipulation, it is necessary to control the input of each trace and manipulate the phase of the microwave inputs, so that this standing wave can be translated. The atom can be trapped in place through this method of wave manipulation. Further adjustment of the wave's frequency and amplitude allows for even more precise modification of the atom's position. Consequently, microwave traces must be coupled to their inputs in a manner that allows adjustment of the wave's frequency, phase, and amplitude.

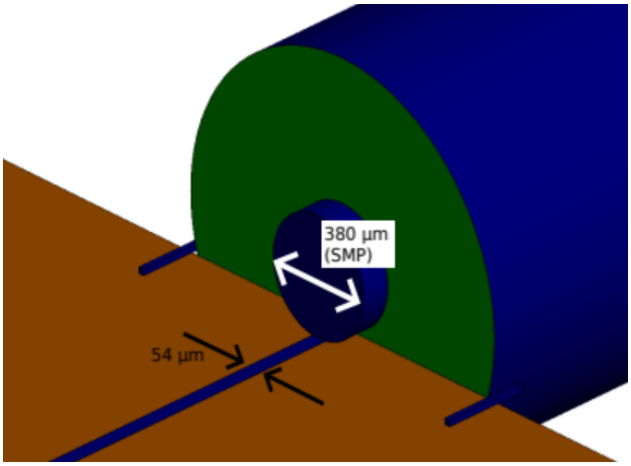

Figure 2.5: FEKO simulation of a coaxial connector directly coupling onto a microwave circuit board. Figure taken from [7].

A solution to this challenge in coupling is to use a tapered wedge coupling component placed at each input of the trace. This component consists of a triangular dielectric wedge of AlON with a triangular copper trace on its surface. This wedge allows a gradual alteration of the trace width and substrate height without unwanted reflections or mode mismatch by preserving the width-to-height ratio of the trace and substrate throughout the wedge geometry. The wedge component is designed to match the coaxial connector's 50 Ω impedance at its widest edge and to transition the mode to one that matches that of the trace. This will allow broadband coupling between the coaxial connector and the microwave trace. While the board substrate cannot be penetrated, glue can be applied manually if and only if the parts are held rigidly and kept stationary during contact. To properly handle these constraints, a micromanipulation device, Scorpion, was developed, enabling three-axis control of microwave circuit components.

2.2 Governing Physics

Microwaves are injected into each trace, generating confined electromagnetic near fields. The near field can be used to exert a force on an ultracold atom and trap it in near-field potential minima between the traces. Adjusting the frequency, phase, and amplitude will change the near field and thus the force exerted on the atom, enabling atom interferometry.

For a microwave circuit, changes in height or width of the trace or substrate result in significant discontinuities in impedance and electromagnetic modes. This poses a significant challenge when coupling a 54 μm microwave trace to a 1.15 mm-diameter coaxial cable. The theoretical reflections at the trace inputs can be calculated using the following equation for Γ_L, the reflection coefficient at the load (input).

$$\Gamma_L = \frac{Z_L - Z_0}{Z_L + Z_0} \tag{2.2}$$

Here, Z_L is the load impedance, and Z_0 is the characteristic impedance of the microwave trace. In a well-designed microwave circuit, both Z_L and Z_0 should be 50 Ω. In the case that Z_L = Z_0, it follows that Γ_L = 0 and there is no reflection. As $Z_L \to \infty$, $\Gamma_L \to$ 1, corresponding to 100% reflection. Physically, this indicates maximum voltage and zero current at the load. If Z_L = 0, Γ_L = -1, which also corresponds to 100% reflection, but with inverted voltage. This indicates there is zero voltage and maximum current at the load. In both cases, a standing wave is formed. The load impedance is determined by the microwave input from the amplifier (via a coaxial cable). The characteristic impedance of the trace, Z_0, is determined by the trace width, substrate thickness, and dielectric constant.

A tapered wedge is used to ensure effective coupling between the coaxial cable input and the microwave trace. This enables broadband transmission.

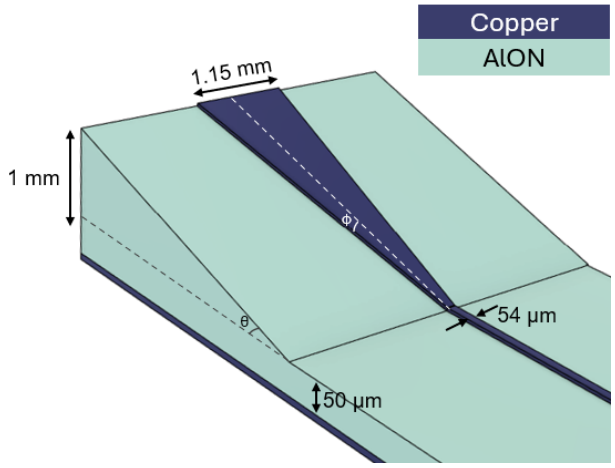

Figure 2.6: Tapered wedge and trace aligned with microwave transmission line.

For impedance and electromagnetic mode to remain consistent along this wedge, the same width-to-height ratio (referring to the trace width and substrate height) must be maintained as in the planar circuit. To achieve this, the angle of the copper trace's taper is made to match that of the substrate wedge angle, so that θ = ϕ.

To ensure proper alignment between the copper trace on the wedge and on the microwave circuit board, it is necessary to control motion and placement in the lateral (x), longitudinal (y), vertical (z), and rotational (α) directions, as shown in Figure 2.6.

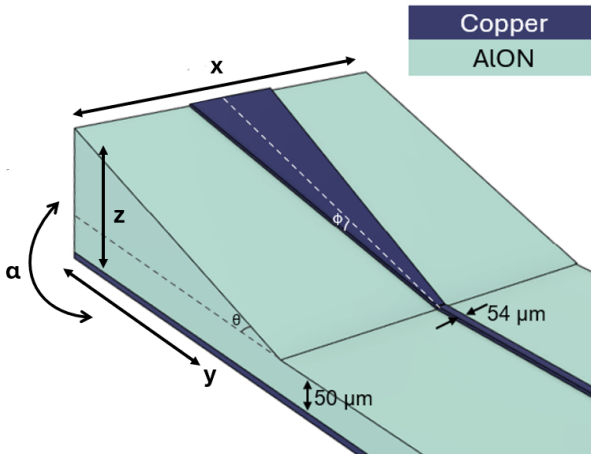

Figure 2.7: Tapered wedge and trace aligned with microwave transmission line, with directions of interest for positioning control labeled.

2.3 Assumptions

Assuming ideal coupling is achievable and the geometry changes minimally with the addition of adhesive, the placement of the wedge should enable a repeatable, low-reflection transition between the coaxial connector and the microwave trace by maintaining impedance matching and minimizing electromagnetic mode discontinuities across the coupling region.

Chapter 3

Methodology

3.1 System Overview

Mechanically, the assembly includes a suction gripper mounted onto a stepper motor-controlled gantry system, which provides movement and coarse position adjustment in the lateral (x) and vertical (z) directions. The microwave circuit board is mounted on a translation stage, with gears on the turning knobs of its vernier micrometers. These gears are paired with gears attached to stepper motors that turn the translation stage knobs. This provides fine position adjustment in the lateral (x) and longitudinal (y) directions.

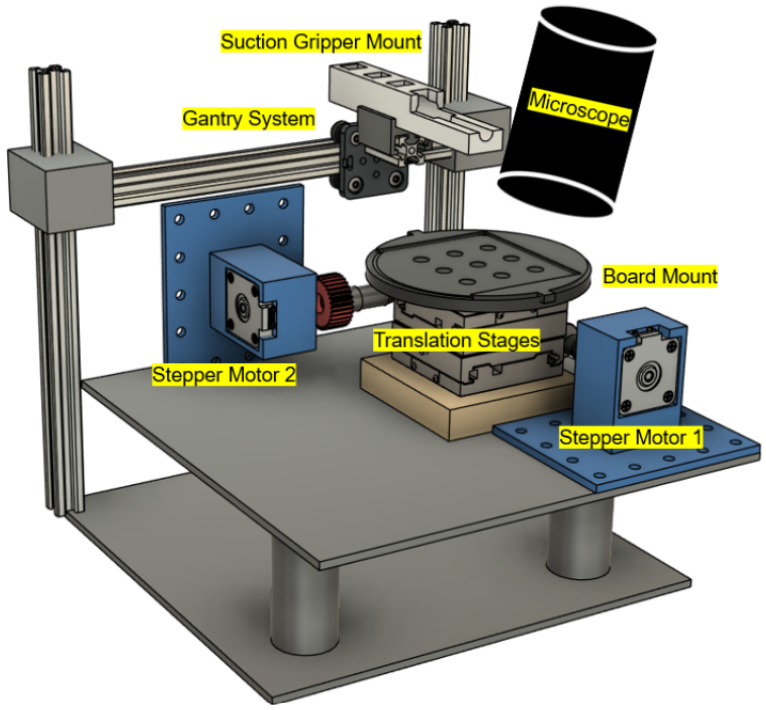

Figure 3.1: Full labeled diagram of microwave atom chip assembly system under the microscope.

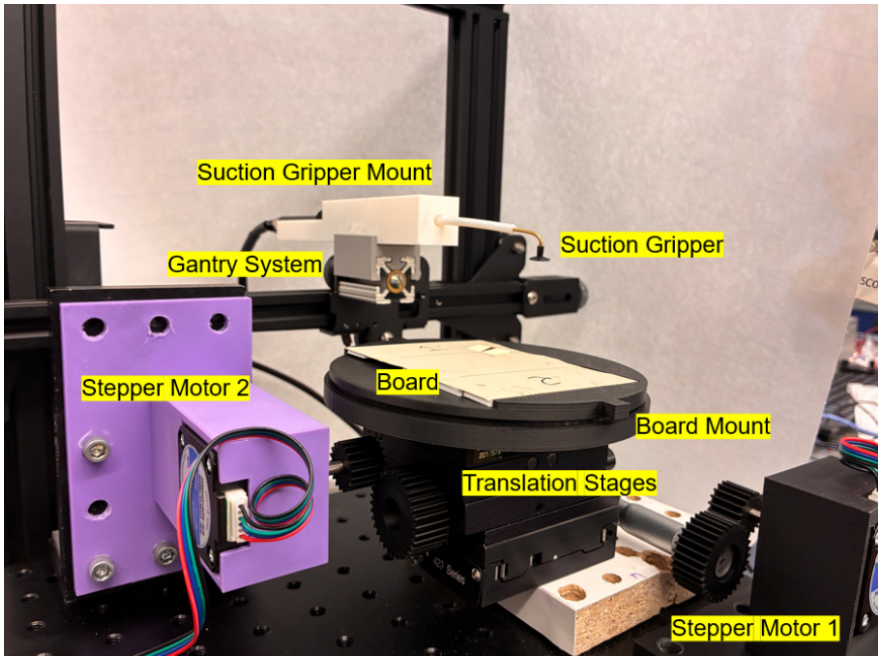

Figure 3.2: Labeled microwave atom chip assembly system with pneumatic suction gripping mechanism, gantry system, and dual motorized translation stages.

3.1.1 Build Process

First Iteration: Claw

For the first claw design, a screw-operated, vice-style gripper was developed and latched onto the wedge. This design succeeded in lifting and moving the wedge; however, the rigid motion and release mechanism caused significant shifting of the wedge's position during placement. The claw's large size relative to the wedge also posed challenges for positioning. For this reason, a design with more flexible, tendon-like motion and a smaller footprint was implemented.

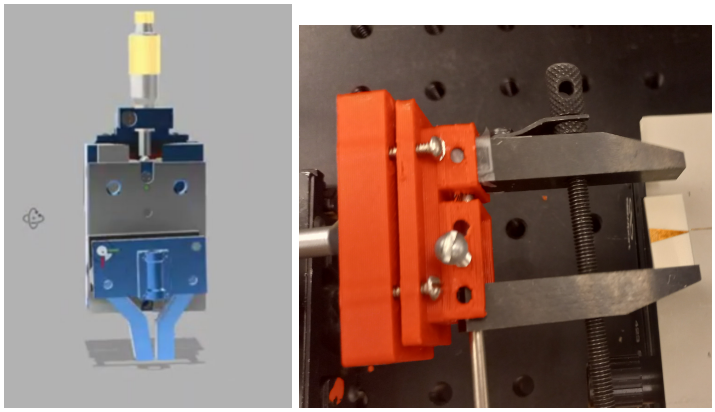

Figure 3.3: CAD model rendering (left) and constructed prototype (right) of the micromanipulation claw attached to the translation stage.

Second Iteration: Finger

The second design iteration is a biologically-inspired mechanism, which was determined to be better suited for adhesion application. This prototype for a gluing system was made using a tendon-like "finger" design.

In this mechanism, two 3mm hollow aluminum pipes are separated by a 3mm aluminum spring. At the end of one pipe, a rubber cap is placed, and a copper wire is sewn through it, running through the pipe and attaching to a 9g microservo. The rotation of the microservo induces tension in the wire, pulling the far-end pipe towards the direction of tension and causing a compressive force on the spring in the same direction. This is the same action a tendon does to a bone in a human finger. The flexor tendons pull on the distal phalanx to initiate joint flexion. By using the aluminum spring as a passive return force, analogous to the role of antagonistic extensor muscles in the human hand, the finger resets its position once the servo releases tension.

While effective in its tendon-like motion, the finger system required at least two such fingers, and it was unclear how well it would maintain its grip on the wedge during motion. However, the top-down "finger down" motion inspired examination of a system that could both hold and move the wedge with just one "finger". This resulted in the final design, the suction gripper.

The finger mechanism currently serves as a prototype for a gluing mechanism. A needle can be attached to the end of this "finger" to apply adhesive to the components once they are held in place. The back-and-forth motion provided by the tendon-like movement spreads this adhesive in a neat line.

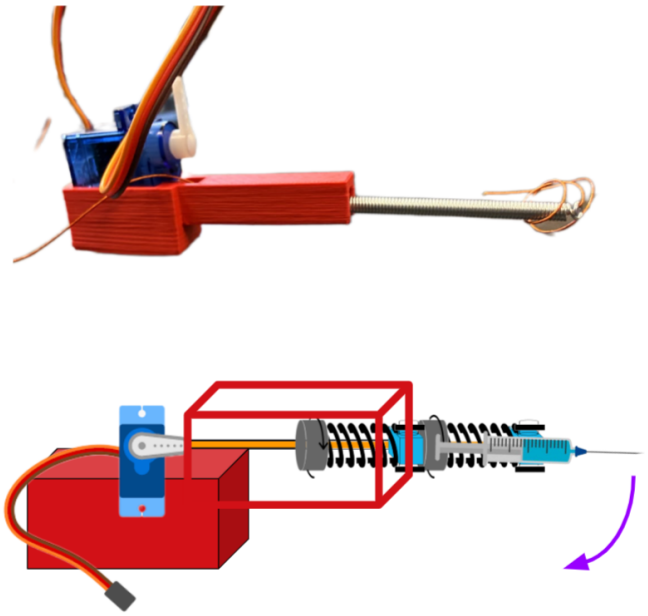

Figure 3.4: Image of "finger" mechanism prototype with spring threaded with wire for tendon motion (top). Diagram of envisioned "finger" gluing mechanism with added syringe for adhesive application (bottom). Microservo in blue, 3D printed casing in red.

Final Iteration: Suction

In addition to gripper-like devices, vacuum holding was explored, as this method is common in surface-mounting devices. These methods showed the most promise for larger-scale applications.

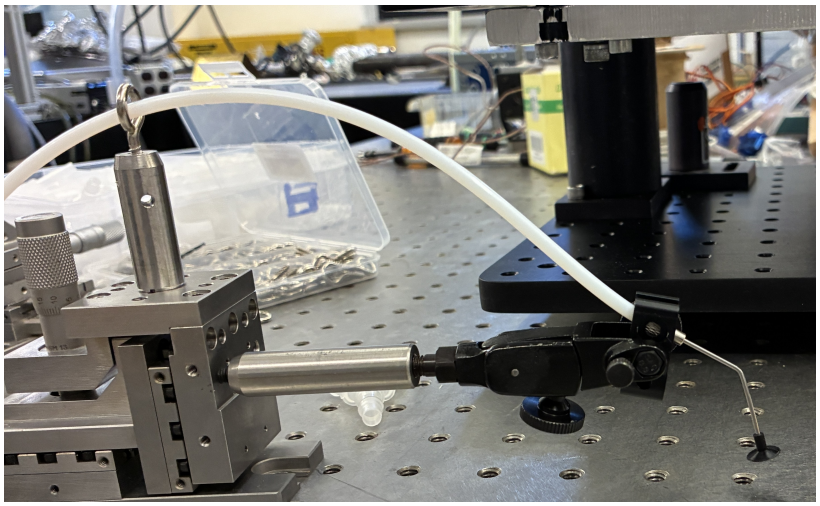

Figure 3.5: Vacuum-driven pick-and-place tool comprised of a metal pipe, capped with a suction cup, led by hollow plastic tubing through a translation stage.

3.2 Detailed Design

The final assembled device includes three main systems. These are the suction gripper, to hold onto components; the gantry system, for coarse control in the x and z directions; and the motorized translation stage assembly, for fine control in the x and y directions (with additional coarse rotational control provided by the board mount). These systems are assembled on two stacked aluminum optical breadboards positioned under an optical microscope. The breadboards are stacked so that the end of the top board is offset from the end of the bottom board, creating space for mounting the gantry system to the bottom board. The suction gripper is mounted onto the gantry system. The motorized translation stage is mounted onto the top optical board, directly under the optical microscope. This system is pictured in Figure 3.6.

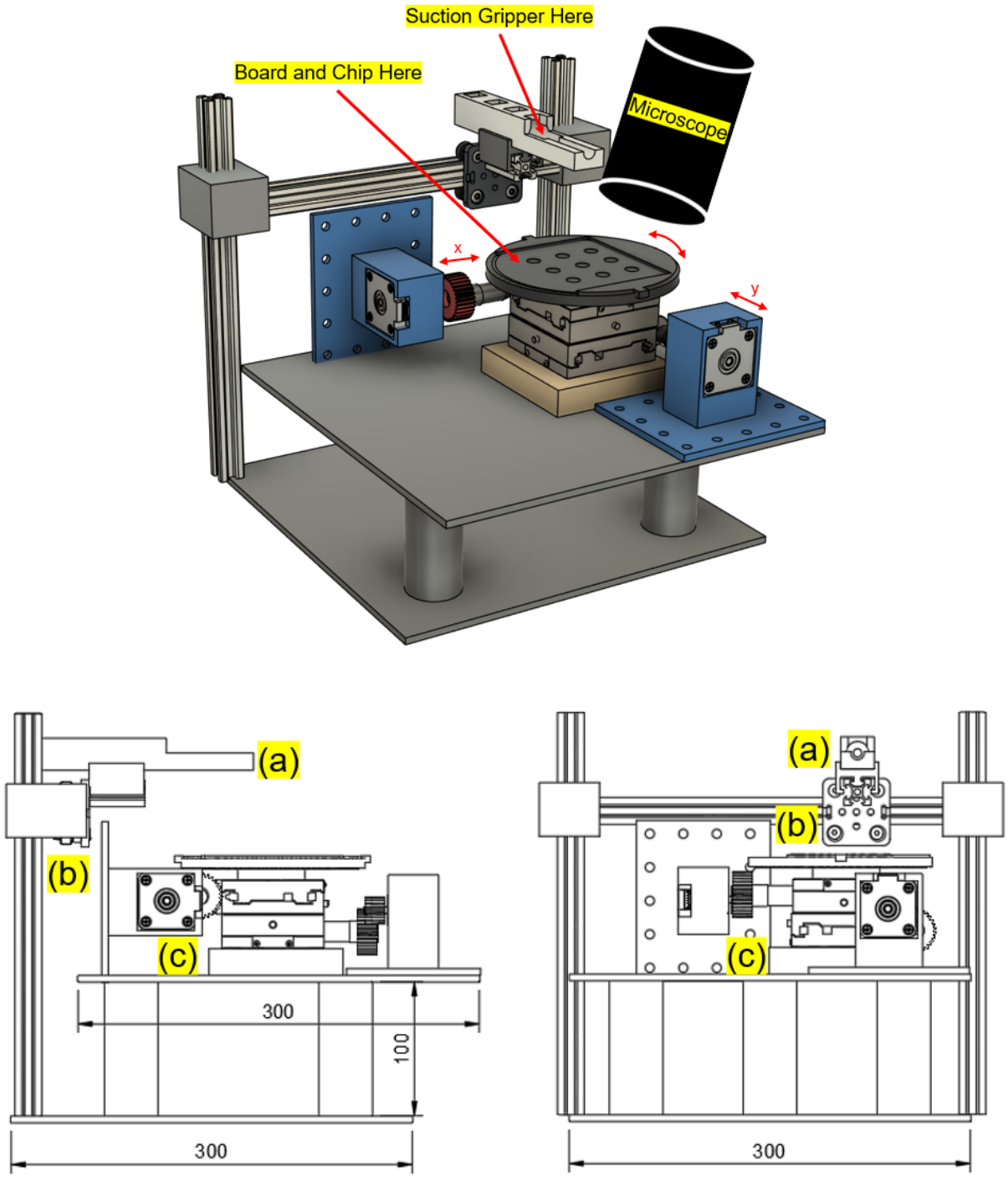

Figure 3.6: CAD model (top) and technical drawing (bottom) of microwave chip assembly system. The assembly model includes a pneumatic suction gripper mount (a), a gantry system (b), and dual motorized translation stages to control stage mvoement in x and y directions (c). All dimensions are given in millimeters.

3.2.1 Suction Gripper

The suction gripper is built around a vacuum pick-and-place tool, which is mounted on the gantry system and connected to a compressed-air system. The mounting is done via two 3D-printed pieces, the first of which ("suction gripper mount") holds the pick-and-place tool, and the second of which ("suction-to-gantry mount") fastens the first piece to a section of V-Slot 20x20mm linear rail that is screwed into the gantry system. The suction mechanism uses a brass pipe bent to a perpendicular angle with a suction cup at its end, attached to the pickup tool via plastic sheathing. This allows the tool to enter from the horizontal direction, avoiding any interference with the microscope above the system. When the suction cup at the end of the tool makes firm contact with the component being moved, the compressed air traveling through the system creates a region of low pressure beneath the suction cup. Then, the higher external pressure of the surrounding air pushes the component to the cup, allowing it to be held and lifted.

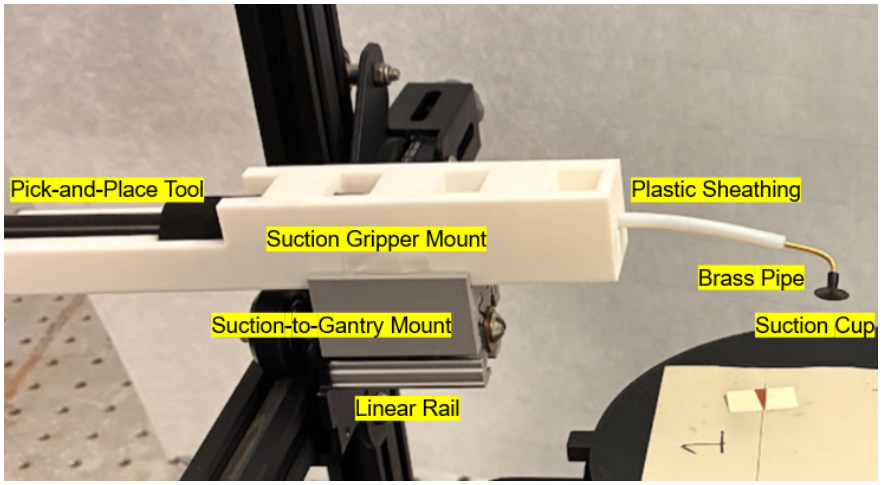

Figure 3.7: Suction gripper in assembly.

The suction gripper is mounted to the gantry system via a 3D-printed mount, which is custom-designed to fit the exact specifications of the pickup tool and attached piping.

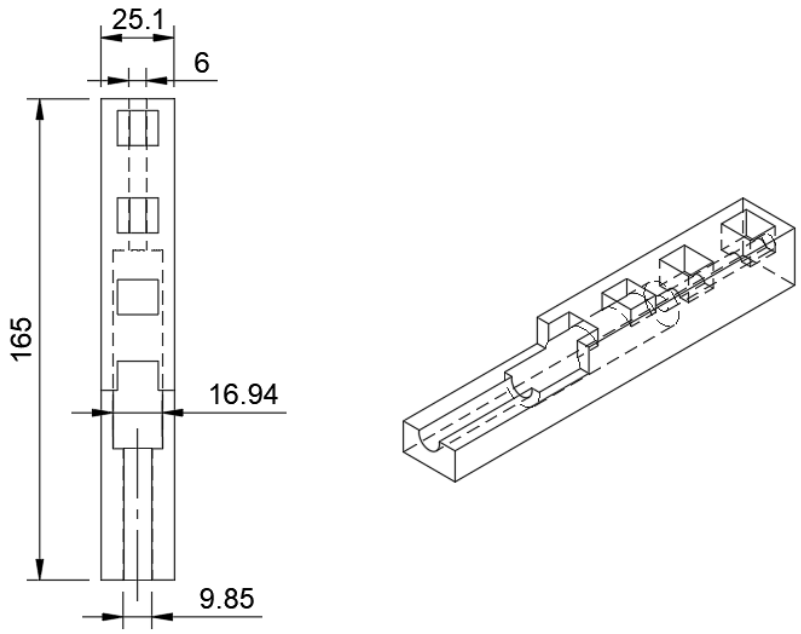

Figure 3.8: Technical drawing of suction gripper mount. All dimensions given in millimeters.

3.2.2 Gantry System

A gantry system (Fig. 3.9) is used to control the position of the suction gripper. A stepper motor at the base of the gantry system moves the suction gripper up and down. A stepper motor at the side of the gantry system is used to move the suction gripper side-to-side laterally. This allows the wedge component to be picked up and moved around on the board with coarse motor control. An Arduino Uno R3 microcontroller and associated code are used to correlate the up, down, and side-to-side motions to the arrow keys on a computer keyboard for ease of user control (Appendix A.2).

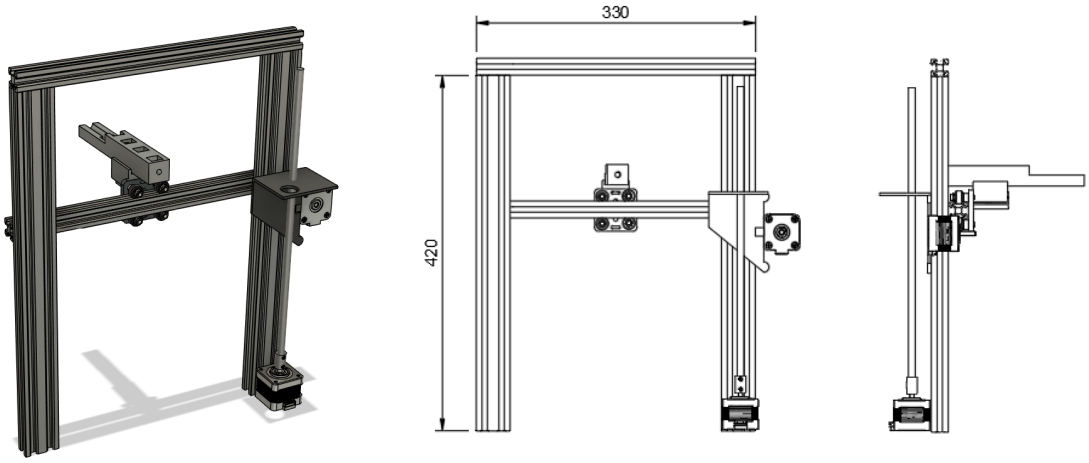

Figure 3.9: CAD model (left) and technical drawing (right) of gantry system used to move suction gripper. The vertical linear rails are 20x40mm V-Slot. The horizontal linear rail is 20x20mm V-Slot. All dimensions are given in millimeters.

3.2.3 Motorized Translation Stage

A stacked translation stage system (Fig. 3.10) is used to control the position of the microwave circuit board. Two translation stages are used to move the board in the x and y directions. This system allows further fine positioning after the coarse positioning provided by the gantry system, along with an extra lateral axis of motion.

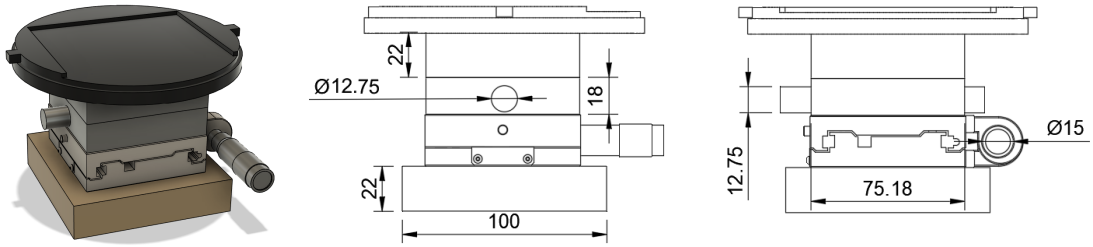

Figure 3.10: CAD model (left) and technical drawing (right) of the translation stage used to move the circuit board. From bottom to top, the assembly consists of: a 22 mm spacer, the first (x-direction) translation stage, the second (y-direction) translation stage, another 22 mm spacer, and the board mount. All dimensions are given in millimeters.

The board itself is placed in a mount on top of the stacked translation stages. This mount is made in two parts. Its bottom section is fixed to the translation stage via 1/4"-20 screws and features a circular slot along its inner circumference (Fig. 3.11).

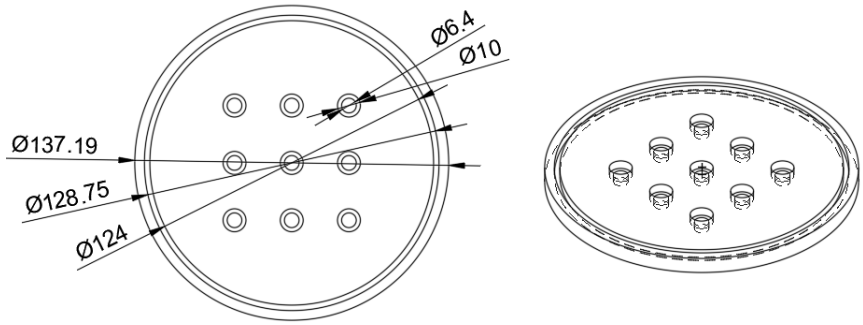

Figure 3.11: Technical drawing of the bottom (fixed) section of the board mount with circular slot along its inner circumference. This piece is fixed to the topmost spacer using 1/4"-20 screws. All dimensions are given in millimeters.

The top section of the board mount has a raised ledge along the inside of its circumference, which fits loosely into the slot in the bottom part, allowing manual rotation of the part (fig. 3.12).

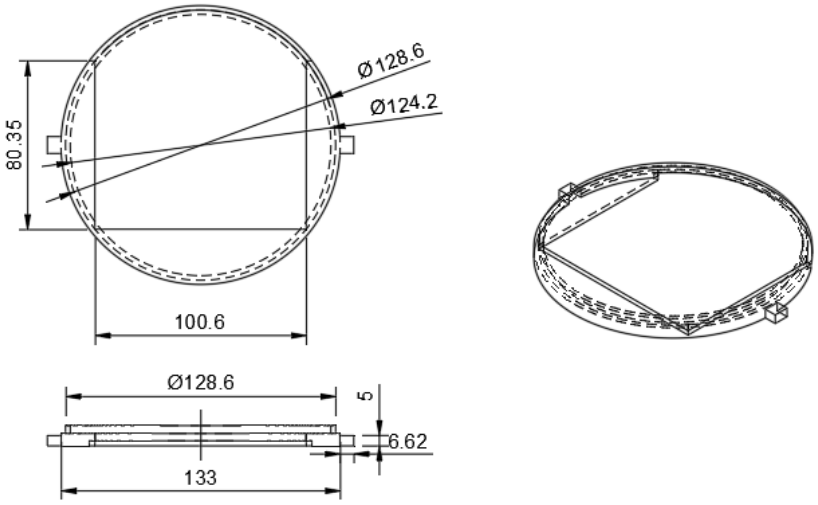

Figure 3.12: Technical drawing of top (rotating) section of board mount with raised bottom ledge that slots into circular slot of bottom section of board mount. All dimensions are given in millimeters.

Each of the two knobs on the stacked translation stages is driven by a stepper motor. The stepper motors are mounted to the optical board using 3D-printed mounts (fig. 3.13 and 3.14). An Arduino Uno R3 microcontroller and associated code are used to correlate the motion of the translation stages to the W, A, S, and D keys on a computer keyboard for ease of user control (Appendix A.2).

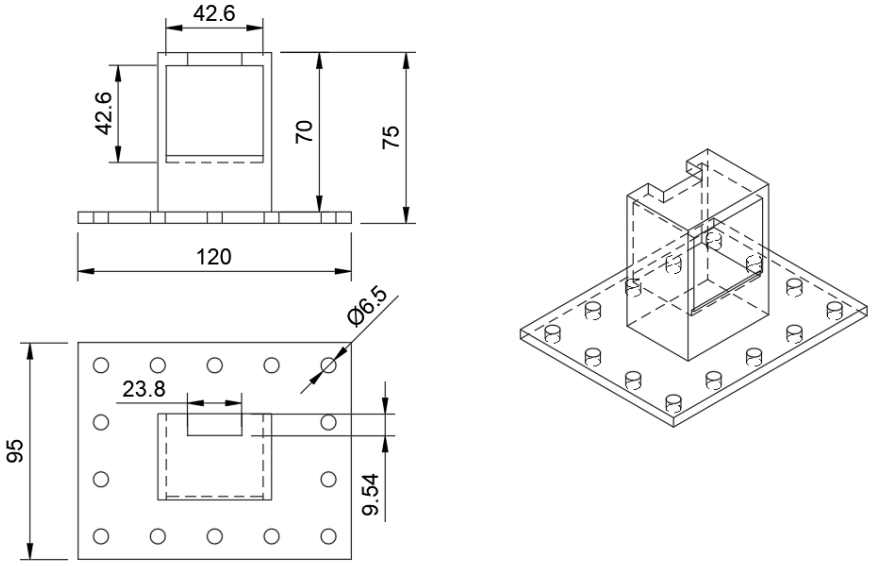

Figure 3.13: Technical drawing of motor mount used to position motors in line with the knob from the y-direction translation stage. The mount is fixed to the optical board using 1/4"-20 screws. All dimensions are given in millimeters.

This motor mount, used to position the motor shaft in line with the knob of the x-direction translation stage, is fixed to an optical vertical mount screwed into the optical board, so that the motor mount is oriented sideways (Fig. 3.2).

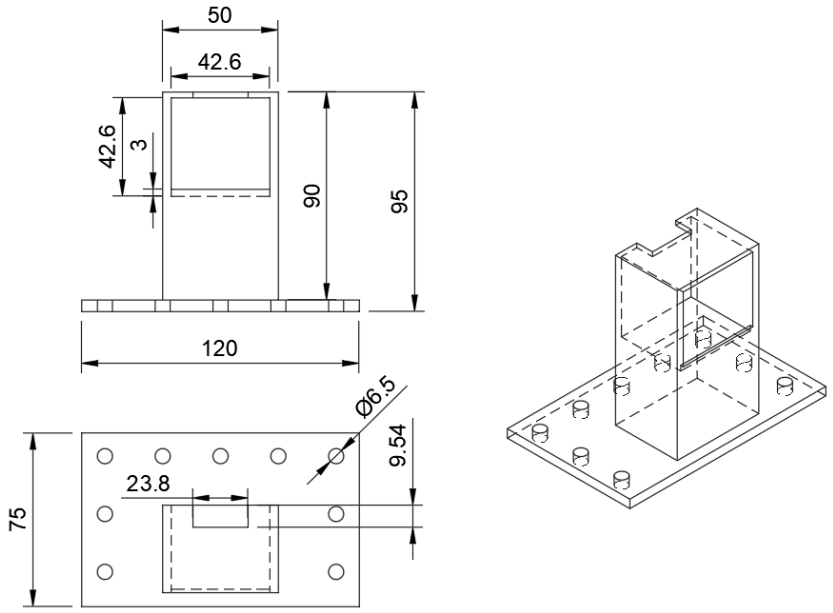

Figure 3.14: Technical drawing of motor mount used to position motors in line with the knob from the x-direction translation stage. 1/4"-20 screws are used for all mounting. All dimensions are given in millimeters.

A 3D-printed 18-tooth gear is fitted onto the shaft of each stepper motor. This gear is interlocked with a 3D-printed 32-tooth gear fitted to the knob of the translation stage. The combination of both gears resulted in a 1.78:1 (16:9) gear ratio, with an output speed of 0.5625 times the stepper speed and a torque increase of about 1.78 N·m relative to the stepper, ignoring losses. In this way, the stepper motors can operate the translation stages. It was found that 1 full rotation of the smaller gear fixed to the motor shaft yields 1 mm in translation stage displacement. For specfic resolution and error details see Error Sources and Uncertainty.

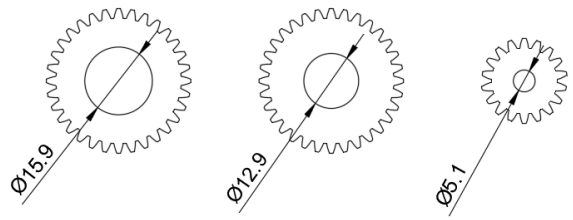

Figure 3.15: Technical drawing of gears connecting motors with knobs of the translation stage. From left to right: gear fitting to micrometer knob of bottom-most translation stage, gear fitting to knob of top-most translation stage, gear fitting to motor shaft. All gears have a 16:9 gear ratio. All dimensions are given in millimeters.

3.3 Apparatus and Materials

The key components used in this assembly are detailed in Table 3.1.

Table 3.1: Assembly Components

Component	**Role**	**Specification / Note**	**Estimated Price (USD)**
Newport 3" Translation Stage	Fine x-y board alignment	Existing lab stage	$40
Newport 423 Series 1.0 in. Travel Linear Stage	Fine x-y board alignment	Existing lab stage	$355
SM-25 Vernier Micrometer	Drives Newport 423 series linear stage	Existing lab tool	$166
Coarse support / gantry	Brings actuator into working region	Optical-table posts, mounts, rails	$50
Kobalt QUIET TECH 4.3-Gallon Portable Electric 150 PSI Twin stack Air Compressor	Suction for pickup and hold-down	Compressed-air vacuum line; cup/tubing size under refinement	$250
Bent tube / suction tip	Contact interface to wedge	Brass tube for vacuum	$8
Microservo	Tendon-inspired mechanism actuation	9 g-class	$10
Aluminum tubes and spring	Tendon-inspired prototype structure	3 mm hollow tubes, 3 mm spring	$15
Stepper motors	Motion of gantry system and translation stages	Nema 17, 4 used	$10 ea
Arduino Uno R3 Microcontroller	Operation of stepper motors for gantry and translation stage motion	2 used	$28 ea

3.4 Data Acquisition

Data is collected by attempting to move a sample wedge to the desired position on a microwave circuit board using the device. Then, an image of the wedge on the board is taken using an optical microscope, and the distance of the gap between the ideal alignment and actual alignment is measured from the image. One such measurement is pictured below:

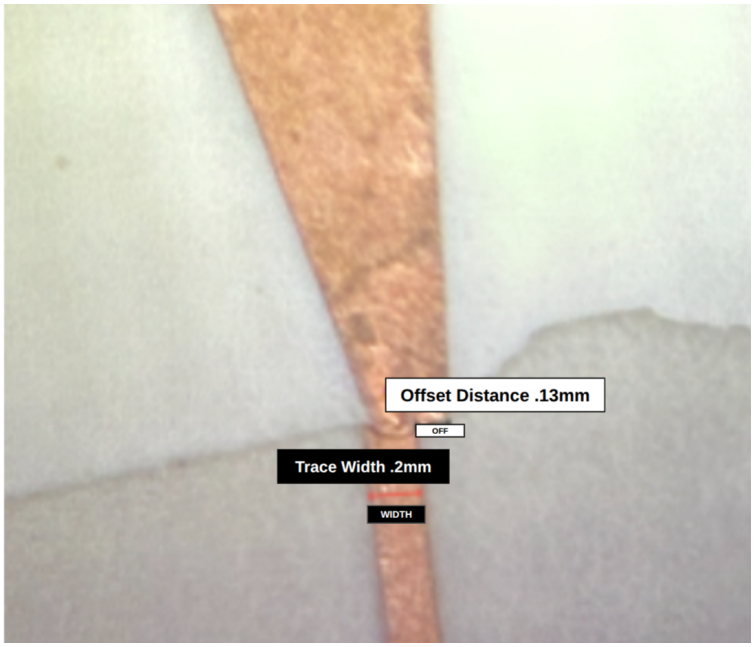

Figure 3.16: Wedge component that has been placed on the microwave circuit board using the atom chip assembly device, with measurements indicating distance from target.

3.5 Experimental Protocol

For each mechanical iteration, the device is tested on a sample wedge and observed under a microscope. The device is used to pick up a sample wedge randomly placed on the board, and then positioned (using the coarse control from the gantry system and the fine control from the motorized translation stage) to best align with the trace on the microwave circuit board. Once aligned, the wedge is released. The alignment between the end of the wedge and the copper trace is checked using the optical microscope, and the efficacy of the manipulation device is assessed.

Chapter 4

Results

The results of the experiment were found through trials and comparisons of three possible actuator routes, as well as specific testing of movement of the system once assembled. Sections 4.1 through 4.3 present the observed behavior and performance of the vice-style claw, tendon-inspired finger, and suction gripper, respectively. Section 4.4 compares these approaches in terms of their practical strengths and limitations, and Section 4.5 identifies the prototype direction selected on the basis of those results. Detailed interpretation and evaluation against the design requirements are presented in Chapter 5.

4.1 Outcome of the Vice-Style Claw

The claw could trap and transport a wedge. It proved that a small stage-mounted mechanism can physically acquire the part.

Its weakness was release. As the wedge was held by rigid contact, opening the jaws disturbed the part when placed. The wedge shifted significantly even when pre-release alignment was correct.

4.2 Outcome of the Tendon-Inspired Finger

The single-axis prototype confirmed that servo tension bends the distal section, and the spring provides return. The compliant motion is softer than the rigid claw.

The tendon system was not fully developed into a primary pickup mechanism during the capstone timeline. It needed further work on mounting, range of motion, and role in the assembly sequence. It was reinterpreted as an auxiliary subsystem suited for adhesive delivery, gentle nudging, or angular correction after the main tool has placed the wedge.

4.3 Outcome of the Suction Gripper

The vacuum-enabled tool successfully lifted, translated, lowered, and maintained hold-down contact after placement. Acting as a temporary hold-down finger during adhesive application.

It was observed that imperfect suction seals or off-center pickup caused wedge rotation or jitter. Hose or mount bias introduced a visible tilt. In some tests, the suction cup geometry was too large for the working region, blocking the microscope view.

Several trials were conducted using the final device, which included the suction gripper design. For each trial, the device was used to place the chip along a copper trace on the microwave circuit board, and then an image taken through an optical microscope was used to determine the distance between the

edge of the narrowest point of the wedge and the nearest edge of the trace. This value, the distance from the target, was used to assess the device's performance. The trials conducted yield the following results (Table 4.1):

Trial	Distance from Target (mm)
1	0.23
2	0.13
3	0.11
4	0.05
5	0.04

Table 4.1: Device Accuracy Across Trials with Standard Deviation 0.076 mm (Section 5.2)

The shortest distance achieved was 40 µm, and the highest distance was 230 µm, showing that there is still great variability between trials. The device can operate on the scale of tens of microns, but is not yet solidly microscale.

4.4 Comparative Summary

Table 4.2 summarizes the three approaches.

Table 4.2: Iteration Comparison

Approach	Strength	Limitation
Vice-style claw	Effective grasp, straightforward pickup	Release disturbed wedge placement
Tendon-inspired compliant tool	Gentle motion; promising for secondary adjustment or adhesive application	Full pickup integration not completed
Suction gripper	Combined pickup, transport, placement, and hold-down in one tool	Sensitive to seal quality, off-center pickup, tilt, and head size

4.5 Prototype Direction

The preferred architecture is a pneumatic pickup tool within a coarse-fine motion system: coarse positioning by the gantry system moving the pickup tool, fine alignment by the linear stage carrying the board. The tendon mechanism will remain as a future adhesive applicator.

Chapter 5

Analysis and Discussion

5.1 Comparison to Theoretical Requirements

The prototype performs best on Δx and Δy control, and the stage-based architecture supports controlled planar alignment under microscope observation. It performs less well on θ and vertical tilt, which still depend on pickup geometry, hose compliance, and manual angular adjustment rather than a dedicated rotational degree of freedom. Hold-down is handled better by the pneumatic tool than by the claw, as the suction head can remain in contact after the wedge reaches the surface.

The final assembly yielded coarse motion in the vertical z direction and alignment in the lateral x and y directions within tens of micrometers. Fine rotational alignment is still not achieved. All motion can still be more granulated to what is theoretically possible and needed for the system.

5.2 Analysis of Suction Gripper System

The pneumatic tool combined pickup and hold-down in one mechanism. In addition to that, it could also be easily assembled from lab-accessible components faster than a multi-finger microgripper, yielding more experimental feedback per iteration.

The positional error of the suction gripper device was recorded over five successive trials (Table 4.1).

From this data, the mean error is given by:

$$\bar{x} = \frac{1}{n}\sum_{i=1}^{n} x_i = 0.112 \text{ mm}$$

Then, 0.112 mm represents the average accuracy of the system.

The standard deviation is given by:

$$\sigma = \sqrt{\frac{1}{n-1}\sum_{i=1}^{n}(x_i - \bar{x})^2} = 0.076 \text{ mm}$$

This indicates that the distance varies from 0.076 mm around the mean.

Both the mean error and standard deviation are greater than where they would ideally be for a micromanipulation device. A challenge of achieving our final goal of aligning a wedge to a 54 μm trace should have both these values in the order of a single micrometer. For the first version of this device, however,

these results are promising. It appears that with greater user practice, the error can be in the low tens of micrometers.

The values given by Table 4.1 are listed in chronological order of trial. Meaning, with each trial, the alignment became better. This can be further quantified by calculating percent error relative to the initial trial:

$$\text{Percent Error} = \frac{E_n}{E_1} \times 100\%$$

where E_n is the error at trial n and E_1 is the error from the first trial.

The resulting percent errors for each Trial n are:

- Trial 1: 100%
- Trial 2: 56.5%
- Trial 3: 47.8%
- Trial 4: 21.7%
- Trial 5: 17.4%

With each subsequent trial, the percent error decreases. This indicates that there is some level of skill involved in the operation of the device. This gradual decrease in error is also likely impacted by the conducting of trials one after the other. A few subsequent attempts at chip placement, with each attempt bringing the chip closer to its ideal position, yields the best alignment.

5.3 Error Sources and Uncertainty

Stepper Resolution Error

Stepper motors have an inherent motion resolution set by the spacing of their internal electromagnets. As a result, their motion occurs in discrete increments rather than as a perfectly continuous displacement. This creates a systematic stepping effect that limits absolute micrometer-scale positioning. Gearing was introduced to reduce this effect, but it could not eliminate it entirely. In this system, the resulting motion resolutions are listed below.

For the translation stage specifically, motion of one tooth on the 18-tooth gear produced approximately 0.056 mm of stage displacement. Based on the specifications of the NEMA 17 stepper motor, one motor step (1.8°) would be expected to produce 0.005 mm of translation-stage motion, measuring 1 mm of travel per 200 motor steps [8].

In practice, however, the system does not move by a fixed amount per key press because the control program is time-dependent: the longer a direction key is held, the farther the stage travels in that direction.

To estimate the displacement associated with a single key press, the key was pressed repeatedly until the 18-tooth gear completed one full rotation. This required approximately 26 key presses.

Using this result,

$$\frac{1 \text{ mm}}{26} \approx 0.038 \text{ mm} = 38\mu\text{m}$$

so a single key press corresponds to an approximate translation-stage displacement of 38 μm.

Axis	Resolution
Gantry Lateral X	1 mm
Gantry Longitudinal Y	1 mm
Stage X	$\sim$40 µm
Stage Y	$\sim$40 µm

To experimentally evaluate this behavior, a needle was attached to the actuator end and measured against a microscope ruler with 0.2 mm divisions. The needle was then driven by a single key press in each direction, and this procedure was repeated 30 times.

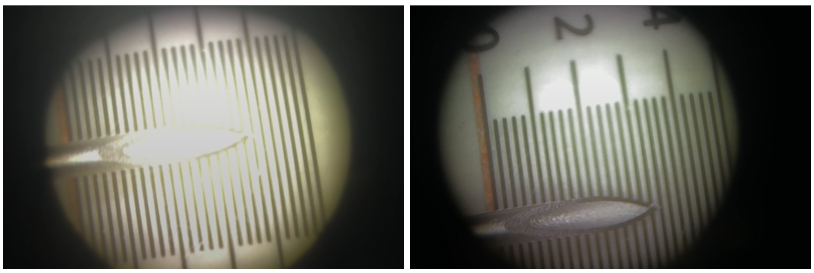

Figure 5.1: Needle positioned against a microscope ruler with 0.2 mm divisions.

5.4 Interpretation

This work began as an open comparison between rigid gripping, compliant gripping, and suction-based pickup. The result was the selection of the suction-based pickup due to its stable release and consistent load. The project has now become a mechanical framework for a dedicated microwave wedge assembly system. We produced a microscope-compatible micromanipulation stage for the microwave circuit boards and wedge components and demonstrated a workable pickup-and-placement sequence.

5.5 Design Iterations and Trade-Offs

Each design iteration experienced its own set of trade-offs and failure modes, which are summarized in Table 5.1.

Table 5.1: Observed Failures

Issue	Likely cause	Design implication
Release-induced wedge shift	Abrupt unloading in rigid claw	Avoid rigid opening during final placement
Wedge rotation/jitter during suction	Off-center pickup, cut suction cup, or air leak	Improve seal quality and pickup-head symmetry
Tilted approach	Hose stiffness, mount compliance, or oversized assembly	Shorten/soften pickup path; add angular adjustment
Motion overshoot after stop	Stage inertia and discrete step commands	Quantify drift; add damped or closed-loop control
Poor visibility near work zone	Pickup head too large for target scale	Shrink suction interface; improve optical access

The rigid claw showed that strong grasping does not ensure stable placement. The tendon prototype showed that compliance is useful, but it better fits a secondary role. The pneumatic tool showed that the best pickup mechanism can also serve as the hold-down mechanism.

An articulated arm would have been harder to calibrate, more likely to obstruct the microscope, and slower to build. The Cartesian gantry strategy was more controlled and readily producible from available parts.

5.6 Limitations

- No finished adhesive-delivery subsystem.
- No fine rotational adjustment.
- Not automated: microscope is human-observation only, with no image-based feedback. Final alignment depends solely on operator judgment.
- No microwave input validation yet.

Chapter 6

Conclusion and Future Work

6.1 Summary of Contributions

This thesis presented Scorpion, a microscope-compatible micromanipulation platform for tapered wedge placement in microwave atom-chip assembly.

Three design iterations were built and compared. The vice-style claw achieved pickup but introduced release disturbance. The tendon-inspired concept demonstrated a gentle motion suited for adhesive delivery or fine adjustment. The pneumatic pickup provided the best combination of pickup, placement, and hold-down and became the preferred direction.

6.2 Assessment Against Objectives

Table 6.1 summarizes the objective status.

Table 6.1: Objective Assessment

Objective	Status	Assessment
Define placement variables and system requirements	Met	Identified critical geometric variables and requirements for pickup, alignment, angular control, and hold-down.
Compare multiple actuator concepts	Met	Three concepts built or prototyped; strengths and weaknesses compared.
Integrate a microscope-compatible motion platform	Met	Architecture combines stage-based fine motion, swappable actuator, and microscope access.

6.3 Broader Impact

Many research labs face microassembly problems. Scorpion shows how a lab can address that gap with modular hardware, microscope-guided alignment, and application-specific actuators. This approach can be applied to microwave atom chips, quantum devices, microelectronics, and research instrumentation.

6.4 Future Work

1. **Reduce and stiffen the pneumatic pickup geometry.** A smaller interface and better-constrained hose path will reduce tilt and improve microscope visibility.
2. **Improve resolution of motion from tens of micrometers to micrometers.** An improvement in overall resolution can be afiner-toothedgh finer ta oothed geathe rs or change in motor used (miniature steppers or linear actuators). Resoluld also significantly gresimplymprove by merely reducing jitter in the current system.
3. **Use tendon design as adhesion tool.** This device can be used for adhesive deposition, as well as edge nudging and orientation correction while the pneumatic head holds the wedge.
4. **Incorporate fine rotational position control.** Fine rotational control can be achieved through the incorporation of a motor-controlled rotation stage.
5. **Integrate microscope camera and image-based alignment.** Implement computer vision for precise alignment.

Bibliography

[1] Hao, Yufei, et al. “Universal Soft Pneumatic Robotic Gripper with Variable Effective Length.” *Proceedings of the 35th Chinese Control Conference (CCC)*, 27–29 July 2016, Chengdu, China, IEEE, 2016, pp. 6109–6114. https://doi.org/10.1109/ChiCC.2016.7554316

[2] Xie, Zhexin, et al. “A Proprioceptive Soft Tentacle Gripper Based on Crosswise Stretchable Sensors.” *IEEE/ASME Transactions on Mechatronics*, 2020. https://doi.org/10.1109/TMECH.2020.2993258

[3] Moritoki, Yukihito, et al. “3D-Printed Micro-Tweezers with a Compliant Mechanism Designed Using Topology Optimization.” *Micromachines*, vol. 12, 2021, article 579. https://doi.org/10.3390/mi12050579

[4] Pandya, Abhilash. “ChatGPT-Enabled daVinci Surgical Robot Prototype: Advancements and Limitations.” *Robotics*, vol. 12, no. 4, 2023, article 97. https://doi.org/10.3390/robotics12040097

[5] Xu, Jiang, et al. “OPAM, an Open Source, 3D-Printed Low-Cost Micro-Manipulator for Single Cell Manipulation.” *bioRxiv*, 10 Aug. 2021. https://doi.org/10.1101/2021.08.09.455588

[6] Liao, Hsien-Shun, et al. “Low-Cost, Open-Source XYZ Nanopositioner for High-Precision Analytical Applications.” *HardwareX*, vol. 11, 2022, article e00317. https://doi.org/10.1016/j.ohx.2022.e00317

[7] Miyahira, William, et al. “Microwave Atom Chip Design.” *Atoms*, vol. 9, 2021, article 54. https://doi.org/10.3390/atoms9030054

[8] STEPPERONLINE. “17HS19-2004S1 Stepper Motor Datasheet.” 30 Oct. 2020. https://www.omc-stepperonline.com/download/17HS19-2004S1.pdf

Appendix A

Wiring Manual

The wiring procedure connects the Raspberry Pi, two Arduino Uno R3 microcontrollers, two HW-130 motor shields, four stepper motors, two external motor-power battery packs, and the pneumatic pickup system. The completed wiring supports motorized motion of the gantry and translation-stage subsystems while maintaining separate power for logic control and motor actuation.

Required Materials

Component	Quantity	Purpose
Raspberry Pi 4 or newer	1	Runs the user-control program and communicates with the Arduino boards.
Arduino Uno R3	2	Provides motor-control signals for the HW-130 shields.
HW-130 motor shield	2	Drives the four stepper motors through the M1–M4 motor terminals.
Stepper motor	4	Actuates the gantry and translation-stage mechanisms.
6 V battery pack	2	Provides external motor power, one supply per HW-130 shield.
Male-to-female jumper wires, motor-current rated	20	Connects each stepper motor lead to the shield motor terminals.
Male-to-male jumper wires, motor-current rated	4	Connects each battery pack to the external-power terminals on each shield.
USB A-to-B Arduino cable	2	Connects each Arduino Uno to the Raspberry Pi.
3 A Raspberry Pi power supply	1	Powers the Raspberry Pi.
Kobalt QUIET TECH compressed-air system	1	Provides air supply for the pneumatic suction pickup tool.
USB keyboard and mouse	Optional	Used for direct Raspberry Pi control during testing.

Table A.1: Required wiring and control materials for the Scorpion system.

Safety and Handling Notes

Before wiring the system, disconnect all power sources. Do not insert or remove motor wires while the Arduino, motor shield, or battery pack is powered. Check the polarity of each 6 V battery pack before connecting it to the

HW-130 external-power terminal. The red lead should connect to the positive terminal, and the black lead should connect to ground. Reversed polarity can damage the motor shield or microcontroller.

The motors should not be powered from the Raspberry Pi or Arduino USB connection. USB power is used only for logic and communication. The stepper motors require the separate 6 V battery packs connected to the external-power inputs on the HW-130 shields.

System Layout

The wiring is divided into two identical motor-control units, as shown in Figure A.1. Each unit contains one Arduino Uno R3, one HW-130 shield, one 6 V battery pack, and two stepper motors. One unit controls the gantry subsystem, and the second unit controls the motorized translation-stage subsystem.

Control Unit	Motors Driven	Function
Arduino/HW-130 Unit A	Gantry stepper motors	Provides coarse motion of the pickup tool, including vertical and lateral positioning.
Arduino/HW-130 Unit B	Translation-stage stepper motors	Provides fine x-y positioning of the circuit-board stage.

Table A.2: Recommended division of the two motor-control units.

Label the two Arduino/HW-130 assemblies before wiring. Suggested labels are *Gantry Control* and *Stage Control*. Labeling prevents the motor cables from being accidentally swapped during troubleshooting or reassembly.

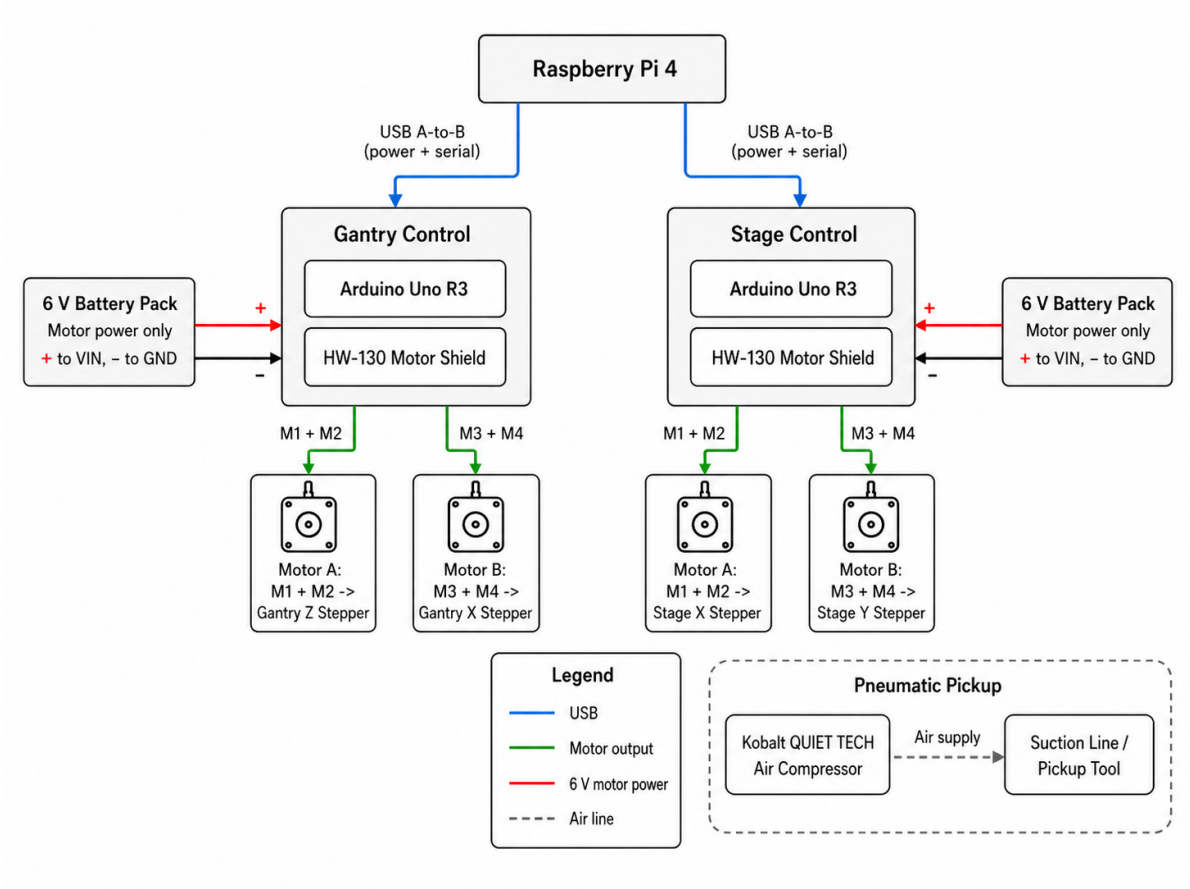

Figure A.1: Overall wiring schematic for the motor-control, power, and pneumatic subsystems.

Assembly Procedure

1. Mount the Motor Shields

Place one HW-130 motor shield on top of each Arduino Uno R3. Align the shield headers with the Arduino headers before pressing the shield into place. Confirm that the shield is seated evenly and that no pins are bent or offset.

2. Connect the Arduino Boards to the Raspberry Pi

Connect each Arduino Uno to the Raspberry Pi using a USB A-to-B cable. These USB connections allow the Raspberry Pi to send keyboard-based motion commands to the Arduino motor-control programs. The USB cables also provide logic power to the Arduino boards.

3. Connect the Stepper Motors

Each HW-130 shield can drive two four-wire stepper motors. A single stepper motor should use two adjacent motor outputs: one motor connects across M1 and M2, and the second motor connects across M3 and M4. Each motor has two internal coils, so the coil pairs must be kept together.

For each stepper motor:

1. Identify the two coil pairs using the motor datasheet or a multimeter.
2. Connect the first coil pair to M1 and M2 for the first motor, or to M3 and M4 for the second motor.
3. Connect the second coil pair to the remaining terminals in the same motor group.
4. Tighten each screw terminal so that the conductor is clamped securely.
5. Gently tug each wire to confirm that it is mechanically secure.

If a motor vibrates but does not rotate, one coil pair is likely reversed or mixed with the other coil pair. Power the system off before correcting the wiring.

4. Connect External Motor Power

Connect one 6 V battery pack to the external-power input on each HW-130 shield. The positive battery lead should connect to the positive external-power terminal, and the negative battery lead should connect to ground.

If the shield includes a power-selection jumper, configure it so that motor power comes from the external battery pack rather than from USB. This prevents the motors from drawing current through the Raspberry Pi or Arduino USB connection.

5. Power the Raspberry Pi

Plug the Raspberry Pi into a 3 A power supply. After the Raspberry Pi boots, confirm that both Arduino boards appear as connected USB devices before running the control program.

6. Connect the Pneumatic System

Connect the Kobalt QUIET TECH compressed-air system to the pneumatic pickup line. Check that the tubing is seated firmly and that the suction path is not kinked. Before using the suction gripper near the microwave chip or wedge component, test the suction tool on a noncritical surface to verify pickup and release behavior.

Wiring Verification Checklist

Before operating the system, verify the following:

- Both HW-130 shields are fully seated on their Arduino Uno boards.

- Each Arduino is connected to the Raspberry Pi by USB.
- Each stepper motor is connected to one complete motor-output group: M1–M2 or M3–M4.
- Each 6 V battery pack is connected with correct polarity.
- Motor power is supplied from the external battery packs, not from USB.
- Jumper wires are firmly seated and do not interfere with moving parts.
- The pneumatic tubing is secure and does not pull on the suction gripper.
- The Raspberry Pi, Arduino boards, and motor shields are placed so that cables cannot be caught in the gantry or translation-stage mechanisms.

Reference Wiring Photographs

Figures A.2, A.3, and A.4 show the wiring layout used during assembly. These photographs should be used as visual references for cable routing, motor-shield placement, and battery-pack connection.

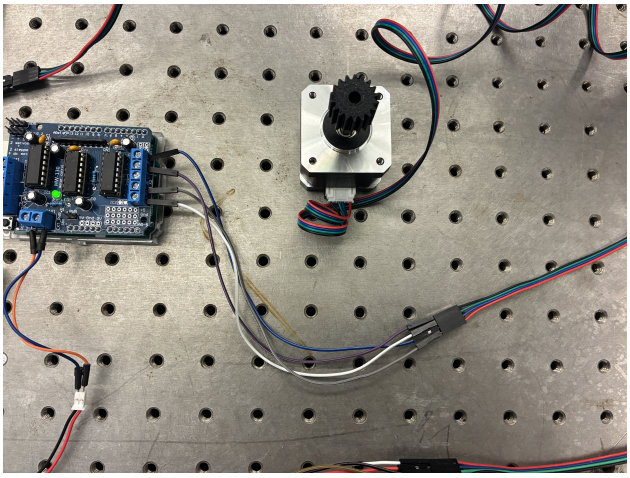

Figure A.2: Close-up view of the HW-130 shield wiring. The stepper-motor leads are connected through the M1–M4 motor-output terminals, and the external motor-power leads are connected at the shield power terminal.

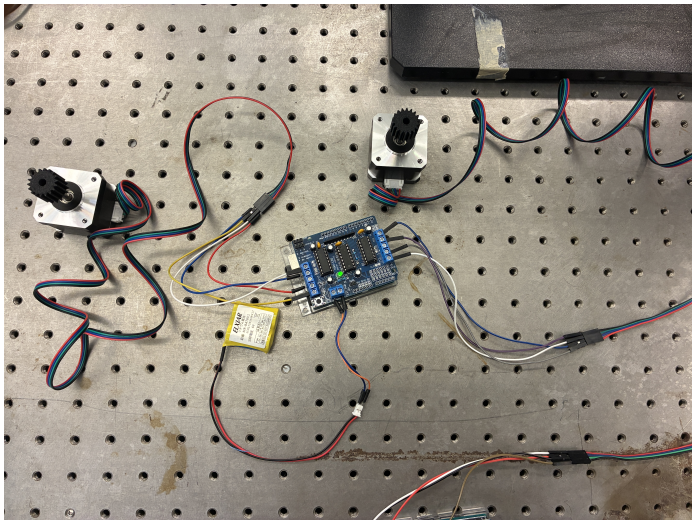

Figure A.3: Two stepper motors connected to one Arduino/HW-130 control unit. The battery pack supplies external motor power

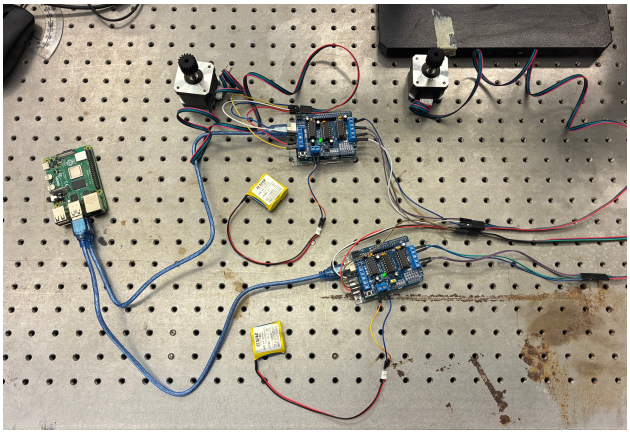

Figure A.4: Full electronics layout with two Arduino/HW-130 control units connected to the Raspberry Pi. This arrangement supports four stepper motors across the gantry and motorized translation-stage subsystems.

Troubleshooting

Problem	Likely Cause	Corrective Action
Motor does not move	External battery is disconnected, discharged, or wired with incorrect polarity	Power off the system, check battery voltage, and reconnect the battery to the shield with correct polarity.
Motor vibrates but does not rotate	Stepper coil pairs are mixed or reversed	Power off the system and verify the coil pairs using the motor datasheet or a multimeter.
Wrong motor moves	Motor cables are connected to the wrong shield or terminal group	Label each motor cable and reconnect it to the intended Arduino/HW-130 unit.
Motion direction is reversed	One motor coil is connected in the opposite order	Reverse the appropriate coil pair or adjust the direction setting in the control code.
Arduino is not detected by Raspberry Pi	USB cable is loose or connected to the wrong port	Reconnect the USB A-to-B cable and restart the control program.
Suction tool does not pick up the wedge	Air line is loose, suction cup is not sealed, or tubing is kinked	Check the tubing path, reseat the suction cup, and test suction away from the chip.

Table A.3: Common wiring and startup issues.

Appendix B

Operation Manual

Operating instructions for the Scorpion microwave atom chip assembly system.

System purpose. The device is used to pick up a tapered wedge, align it with the microwave trace under a microscope, lower it into place, and hold it steady during adhesive application.

Main subsystems.

Subsystem	Function
Suction gripper	Picks up and holds the wedge during transport and placement.
Gantry system	Provides coarse motion of the pickup tool.
Motorized translation stages	Provide fine adjustment of board position.
Microscope	Provides visual feedback for alignment.

Startup.

1. Place circuit board in board mount and place wedge component on top of circuit board.
2. Turn on the microscope illumination and focus on the working region.
3. Connect and verify the suction/air line to the pickup tool.
4. Power the Arduino and motor-control system.
5. Place the board and wedge in the working area under the microscope.
6. Start the motor-control program on the computer.

Keyboard controls.

Input	Action
Arrow keys	Move one motorized subsystem.
W / A / S / D	Move the second motorized subsystem.
1, 2, 3, 4	Change stepping mode: SINGLE, DOUBLE, INTERLEAVE, and MICROSTEP.*
Space	Stop motion and release motors.
Q	Quit the control program.

*A stepper motor has a spinning rotor (usually a permanent magnet) surrounded by several stationary coils. The angular positions the rotor can occupy can be controlled by energizing the coils in different patterns. Stepping mode refers to the current activation of internal coils for the stepper motors.

SINGLE mode energizes one motor coil. This means the rotor jumps from one magnetic pole to the next, yielding rougher motion.

DOUBLE mode energizes two coils simultaneously, allowing the rotor to align between poles. This yields smoother motion and higher torque than SINGLE mode.

INTERLEAVE mode alternates between single and double-coil activation. This allows the rotor to stop at intermediate positions, doubling the resolution.

MCIROSTEP mode drives each coil at varying levels using analog current levels. Instead of being fully ON or OFF, each coil is powered at a certain percentage of the maximum current. This yields finer positioning and continuous torque, with very smooth rotational motion.

Operating procedure.

1. Position the suction cup above the wedge.
2. Lower the pickup tool until the cup seals to the wedge.
3. Lift the wedge slightly and move it over the target trace.
4. Use coarse motion first, then fine stage motion, to align the wedge with the trace.
5. Lower the wedge onto the board and maintain hold-down with suction.
6. Apply adhesive if needed while the wedge is held in position.
7. Release suction only after the wedge remains fixed in place.

Shutdown. Return the system to a safe position, turn off suction, power down the motor-control system.

Appendix C

Code

C.1 Github

The main code used in the model is addressed below. For additional code and further descriptions, access the Atom-chip repository.

C.2 Arduino C Code

```
#include <Wire.h>
#include <Adafruit_MotorShield.h>

Adafruit_MotorShield shield = Adafruit_MotorShield();

// X stepper uses M1 and M2
Adafruit_DCMotor *xCoilA = shield.getMotor(1);
Adafruit_DCMotor *xCoilB = shield.getMotor(2);

// Y stepper uses M3 and M4
Adafruit_DCMotor *yCoilA = shield.getMotor(3);
Adafruit_DCMotor *yCoilB = shield.getMotor(4);

int stepPattern[8][4] = {
  {1, 0, 0, 0},
  {1, 0, 1, 0},
  {0, 0, 1, 0},
  {0, 1, 1, 0},
  {0, 1, 0, 0},
  {0, 1, 0, 1},
  {0, 0, 0, 1},
  {1, 0, 0, 1}
};

int xDirection = 0;
int yDirection = 0;

int xStepNumber = 0;
int yStepNumber = 0;

unsigned long lastXStep = 0;
unsigned long lastYStep = 0;
const unsigned long STEP_DELAY = 7000;  // smaller number = faster

int arrowState = 0;

void setCoil(Adafruit_DCMotor *motor, int forwardOn, int backwardOn) {
  if (forwardOn == 1) {
    motor->run(FORWARD);
  } else if (backwardOn == 1) {
    motor->run(BACKWARD);
  } else {
    motor->run(RELEASE);
  }
}

void useStep(Adafruit_DCMotor *coilA, Adafruit_DCMotor *coilB, int stepNumber) {
  setCoil(coilA, stepPattern[stepNumber][0], stepPattern[stepNumber][1]);
  setCoil(coilB, stepPattern[stepNumber][3], stepPattern[stepNumber][2]);
}

void releaseAllMotors() {
  xCoilA->run(RELEASE);
  xCoilB->run(RELEASE);
  yCoilA->run(RELEASE);
  yCoilB->run(RELEASE);
}

void stopMotors() {
  xDirection = 0;
  yDirection = 0;
```

```
  releaseAllMotors();
}

void readKeys() {
  while (Serial.available() > 0) {
    char key = Serial.read();

    if (arrowState == 1) {
      if (key == '[') {
        arrowState = 2;
      } else {
        arrowState = 0;
      }
    } else if (arrowState == 2) {
      arrowState = 0;

      switch (key) {
        case 'A':
          yDirection = 1;
          break;
        case 'B':
          yDirection = -1;
          break;
        case 'C':
          xDirection = 1;
          break;
        case 'D':
          xDirection = -1;
          break;
      }
    } else if (key == 27) {
      arrowState = 1;
    } else {
      switch (key) {
        case 'w':
        case 'W':
          yDirection = 1;
          break;
        case 's':
        case 'S':
          yDirection = -1;
          break;
        case 'a':
        case 'A':
          xDirection = -1;
          break;
        case 'd':
        case 'D':
          xDirection = 1;
          break;
        case ' ':
          stopMotors();
          break;
      }
    }
  }
}

void moveXOneStep() {
  xStepNumber = xStepNumber + xDirection;

  if (xStepNumber > 7) {
    xStepNumber = 0;
  }

  if (xStepNumber < 0) {
    xStepNumber = 7;
  }

  useStep(xCoilA, xCoilB, xStepNumber);
}

void moveYOneStep() {
  yStepNumber = yStepNumber + yDirection;

  if (yStepNumber > 7) {
    yStepNumber = 0;
  }

  if (yStepNumber < 0) {
    yStepNumber = 7;
  }

  useStep(yCoilA, yCoilB, yStepNumber);
}

void setup() {
  Serial.begin(115200);
  shield.begin();

  xCoilA->setSpeed(255);
```

```
  xCoilB->setSpeed(255);
  yCoilA->setSpeed(255);
  yCoilB->setSpeed(255);

  Serial.println("W/S = Y motor");
  Serial.println("A/D = X motor");
  Serial.println("Arrow keys also work");
  Serial.println("Space = stop");
  Serial.println("Step columns: A, A', B', B");
}

void loop() {
  unsigned long now = micros();

  readKeys();

  if (xDirection != 0) {
    if (now - lastXStep >= STEP_DELAY) {
      moveXOneStep();
      lastXStep = now;
    }
  }

  if (yDirection != 0) {
    if (now - lastYStep >= STEP_DELAY) {
      moveYOneStep();
      lastYStep = now;
    }
  }
}
```